

Soft versus Hard Dynamics for Field-driven Solid-on-Solid Interfaces

P. A. Rikvold^{1,2} and M. Kolesik^{3,4}

¹ Center for Materials Research and Technology, School of Computational Science and Information Technology, and Department of Physics, Florida State University, Tallahassee, Florida 32306-4351

² Department of Fundamental Sciences, Faculty of Integrated Human Studies, Kyoto University, Kyoto 606, Japan

³ Institute of Physics, Slovak Academy of Sciences, Bratislava, Slovak Republic

⁴ Department of Mathematics, University of Arizona, Tucson, Arizona 85721

(February 7, 2020)

Analytical arguments and dynamic Monte Carlo simulations show that the microstructure of field-driven Solid-on-Solid interfaces depends strongly on the dynamics. For nonconservative dynamics with transition rates that factorize into parts dependent only on the changes in interaction energy and field energy, respectively (soft dynamics), the intrinsic interface width is field-independent. For non-factorizing rates, such as the standard Glauber and Metropolis algorithms (hard dynamics), it increases with the field. Consequences for the interface velocity and its anisotropy are discussed.

PACS numbers: 68.35.Ct 75.60.Jk 68.43.Jk 05.10.Ln

Surfaces and interfaces moving under far-from-equilibrium conditions are important in the formation of patterns and structures. For example, domain growth by the motion of defects such as grain boundaries or dislocations influences the mechanical properties of metals [1] and the structures formed during phase transformations in adsorbate systems [2], while the propagation of domain walls influences the switching dynamics of magnetic nanoparticles and ultrathin films [3]. Recently, interface dynamics was even used to analyze the scalability of discrete-event simulations on parallel computers [4]. The importance of moving interfaces in a wide variety of fields has inspired enormous interest in their structure and dynamics [5]. However, despite the fact that many interface properties, such as mobility and chemical activity, depend crucially on the microscopic structure, interest has mostly focused on the large-scale interface structure and its universal properties. In this Letter we show that the microstructure of a moving interface is dramatically influenced by the growth mechanism, with consequences for the interface velocity and its anisotropy.

The detailed microscopic mechanism of the interface motion is usually not known. It is therefore common to mimic the essential features in a dynamic Monte Carlo (MC) simulation of a model stochastic process [1]. In doing so, the first distinction is between dynamics that do not conserve the order parameter, such as the standard Metropolis and Glauber single-spin flip algorithms, and conservative dynamics, such as the Kawasaki spin-exchange dynamic [6]. Once it is decided to which of these two categories the system belongs, it is common to choose the dynamic, largely on the basis of convenience, among the many different forms that obey detailed balance and thus ensure approach to equilibrium.

Here we demonstrate that there can be striking differences between the microstructural consequences of different stochastic dynamics, even among those that obey detailed balance and do not conserve the order parameter.

For this demonstration we use an unrestricted Solid-on-Solid (SOS) interface [7] separating uniform spin-up and spin-down phases in a ferromagnetic $S = 1/2$ Ising system on a square lattice of unit lattice constant. The interface consists of integer-valued steps parallel to the y -direction, $\delta(x) \in \{-\infty, +\infty\}$, where the step position x is also an integer. Its energy is given by the nearest-neighbor Ising Hamiltonian with anisotropic ferromagnetic interactions, J_x and J_y in the x and y direction, respectively: $\mathcal{H} = -\sum_{x,y} s_{x,y} (J_x s_{x+1,y} + J_y s_{x,y+1} + H)$. The two states at site (x, y) are denoted by the spin $s_{x,y} = \pm 1$, $\sum_{x,y}$ runs over all sites, and H is the applied field. We take $s_{x,y} = -1$ on the side of the interface corresponding to large positive y , so that the interface on average moves in the positive y direction for $H > 0$. To restrict the accessible configurations to a simple SOS interface without bubbles or overhangs, transitions are allowed only for spins that have one single broken bond in the y -direction.

Recently [8] we introduced a mean-field approximation for the driven-interface microstructure, in which the probability density function (pdf) for the height of a single step takes the Burton-Cabrera-Frank (BCF) form [7],

$$p[\delta(x)] = Z^{-1} X^{|\delta(x)|} e^{\gamma(\phi)\delta(x)}, \quad (1)$$

where $\gamma(\phi)$ is a Lagrange multiplier which enforces $\langle \delta(x) \rangle = \tan \phi$ independent of x , corresponding to an overall angle ϕ between the interface and the x -axis. The width parameter X , which for a driven interface can depend on both H and the temperature T , is discussed below. The partition function in Eq. (1) is

$$Z = \sum_{\delta=-\infty}^{+\infty} X^{|\delta|} e^{\gamma(\phi)\delta} = \frac{1 - X^2}{1 - 2X \cosh \gamma(\phi) + X^2} \quad (2)$$

with

$$e^{\gamma(\phi)} = \frac{(1+X^2) \tan \phi + \sqrt{(1-X^2)^2 \tan^2 \phi + 4X^2}}{2X(1+\tan \phi)}, \quad (3)$$

where $X_0(T) \equiv e^{-2\beta J_x}$ with $\beta = 1/k_B T$ (k_B is Boltzmann's constant) is the BCF zero-field equilibrium value of X , and $W[\beta \Delta E]$ is the transition probability for a single spin flip which would lead to an energy change ΔE (see [8,9] for details). For $H = 0$, $X(T, H)$ reduces to $X_0(T)$. For instance, using the Glauber transition probability,

$$W_G(s_{x,y} \rightarrow -s_{x,y}) = \frac{e^{-\beta \Delta E}}{1 + e^{-\beta \Delta E}}, \quad (5)$$

we get

$$X_G(T, H) = X_0(T) \left\{ \frac{e^{2\beta J_x} \cosh(2\beta H) + e^{-2\beta J_x}}{e^{-2\beta J_x} \cosh(2\beta H) + e^{2\beta J_x}} \right\}^{1/2}. \quad (6)$$

Equation (5) exemplifies a class of dynamics known as *hard* in the literature on nonequilibrium lattice models [10], in which the transition probabilities depend directly on the total energy change, ΔE . In a different class, known as *soft*, the probabilities factorize into a part due only to the change in the field energy, $\Delta E_H \propto H$, and a part due only to the change in the interaction energy, $\Delta E_J \propto J_x$. One example is the *soft Glauber dynamic*,

$$W_{SG}(s_{x,y} \rightarrow -s_{x,y}) = \frac{e^{-\beta \Delta E_H}}{1 + e^{-\beta \Delta E_H}} \cdot \frac{e^{-\beta \Delta E_J}}{1 + e^{-\beta \Delta E_J}}. \quad (7)$$

It is easy to show that this transition probability also obeys detailed balance.

The important point is that when a factorizing transition probability such as Eq. (7) is used in Eq. (4), all dependence on H cancels due to the detailed balance. Whether one uses a soft or a hard dynamic thus strongly affects the intrinsic interface width and properties that depend on it, such as the propagation velocity. The need to use a soft dynamic in cases where the "field" represents a chemical-potential difference was recognized in some MC studies of three-dimensional crystal growth [11,12].

Next we illustrate the large differences between hard and soft dynamics by comparing analytic approximations and dynamic MC simulations of driven SOS interfaces with $J_x=J_y=J$, using the hard and soft Glauber dynamics, respectively. In particular, we consider the field- and temperature dependencies of the intrinsic interface

For $\phi = 0$, $\gamma(\phi) = 0$, yielding $Z(0) = (1+X)/(1-X)$.

In the approximation of Ref. [8], individual steps are assumed to be statistically independent (like in the original BCF model for *equilibrium* interfaces). The width parameter X is then obtained self-consistently as [8,9]

$$X(T, H) = X_0(T) \left\{ \frac{e^{-2\beta H} W[\beta(-2H - 4J_x)] + e^{2\beta H} W[\beta(+2H - 4J_x)]}{W[\beta(-2H - 4J_x)] + W[\beta(+2H - 4J_x)]} \right\}^{1/2}, \quad (4)$$

width, represented by the average step height, and the resulting interface velocity and its anisotropy.

In Fig. 1 we show numerical evidence supporting our predictions for the average step height, which for $\phi = 0$ is related to X as $\langle |\delta| \rangle = 2X/(1-X^2)$, under both the hard and soft Glauber dynamics at two different temperatures. (Simulational details are given below.) The difference between the step heights for the two dynamics is striking: the results for the soft dynamic are independent of H , in contrast to the strong H -dependence produced by the hard dynamic. Additional confirmation of the functional form of the single-step pdf, Eq. (1), is obtained from the MC data by calculating $\langle |\delta| \rangle$, both directly by summation over the numerically obtained pdf, and from the probability of zero step height for $\phi = 0$ as

$$\langle |\delta| \rangle = \{p[0]^{-1} - p[0]\} / 2. \quad (8)$$

This result is obtained by combining $p[0] = Z^{-1}$ with the above relation for $\langle |\delta| \rangle$ in terms of X .

The spins in an Ising system can be classified by the value of ΔE , which is uniquely determined by s and the number of broken x - and y -bonds. The active spin classes all have one broken y -bond and can be labeled by $s=\pm 1$ and the number of broken x -bonds, $j \in \{0, 1, 2\}$, as js . The classes and corresponding ΔE are given in the first two columns of Table I. The details of our "active-site" implementation of the spin-class based discrete-time n -fold way algorithm [13] are given in Ref. [8], the only difference here being the restriction to flips only at sites with one broken y -bond. The data shown here are for interfaces of size $L_x=10^4$ in the x -direction, which were allowed 5 000 n -fold way updates per active site to reach stationarity, after which pdfs, class populations, and velocities were collected over 50 000 updates per active site.

Assuming up-down symmetry of the interface, the mean perpendicular propagation velocity is given by

$$\langle v_{\perp}(T, H, \phi) \rangle = \cos \phi \sum_j \langle n(js) \rangle \langle v_y(j) \rangle \quad (9)$$

in units of MC steps per site (MCSS). Here, the average spin-class populations, $\langle n(js) \rangle$, are calculated from the single-step pdf, assuming statistical independence [8], and the results are given in the third and fourth columns of Table I. The corresponding contributions to the interface velocity in the y -direction, $\langle v_y(j) \rangle =$

$\{W[\beta\Delta E(j-)] - W[\beta\Delta E(j+)]\}$, are given in the fifth and sixth column of Table I for the hard and soft Glauber dynamic, respectively. The special case of $\phi = 0$ leads to compact formulas:

$$\langle v_{\perp}(T, H, 0) \rangle_{\text{G}} = \frac{\tanh(\beta H)}{(1+X)^2} \left\{ 2X + \frac{1+X^2}{1 + \left[\frac{\sinh(2\beta J_x)}{\cosh(\beta H)} \right]^2} \right\} \quad (10)$$

with X from Eq. (6) for the hard Glauber dynamic, and

$$\langle v_{\perp}(T, H, 0) \rangle_{\text{SG}} = \tanh(\beta H) \frac{X_0}{1+X_0^2} \quad (11)$$

for the soft Glauber dynamic. These results are compared with the corresponding MC data in Fig. 2. The difference between the two dynamics is clear. While the velocity for the hard dynamic approaches unity for strong fields at all temperatures, the soft dynamic yields a velocity which saturates at a smaller, T -dependent value.

The angular dependencies of $\langle v_{\perp} \rangle$ for the two dynamics are illustrated in Fig. 3. The theoretical results represent Eq. (9) with terms from Table I. The hard dynamic yields an anisotropy which changes from that of the single-step model [5] for weak H , to the reverse anisotropy of the Eden model [14,15] for strong H . There is no such change for the soft dynamic, which shows a single-step like anisotropy for all fields. It is likely that the different anisotropies will lead to different growth shapes, as well.

With hard dynamics, the up-down symmetry of the interface is gradually destroyed with increasing field [4,8,9,16], leading to different class populations for $s=+1$ and $s=-1$. Our MC simulations show this skewness to be absent for the soft dynamic. This makes us believe that the field dependence in Eq. (11) is exact in the following sense. If the interface has up-down symmetry and is driven with a soft dynamic, then the generated interface shapes are independent of H . Consequently, the only dependence of the velocity on H is in the difference between the spin-flip probabilities of a down spin and an up spin, which yields $\tanh(\beta H)$ for the Glauber dynamic.

In summary, we have presented analytical and dynamic MC results that show remarkable differences in the microscopic structure of field-driven SOS interfaces, depending on whether the stochastic dynamic is hard (such as the standard Glauber and Metropolis dynamics) or soft. If microstructural information is desired from a dynamic MC simulation, great care must therefore be exercised,

both in choosing the transition probabilities and in interpreting the results. Analogous effects for other models, such as Ising interfaces [8], and in three dimensions, and the possibility that the resulting growth shapes may be different, are left for future study. Further details on the microstructure of the SOS interface under the hard Glauber dynamic will be reported elsewhere [9].

We thank G. Brown, G. Buendia, S. J. Mitchell, M. A. Novotny, and K. Park for useful comments. P. A. R. appreciates hospitality at Kyoto University. Supported in part by NSF Grant No. DMR-9981815, and by Florida State University through MARTECH and CSIT.

- [1] M. I. Mendelev and D. J. Srolovitz, *Acta Mater.* **48**, 3711 (2000); preprint (2001).
- [2] G. Brown, P. A. Rikvold, M. A. Novotny, and A. Wieckowski, *J. Electrochem. Soc.* **146**, 1035 (1999).
- [3] M. A. Novotny and P. A. Rikvold, in *Encyclopedia of Electrical and Electronics Engineering*, Vol. 12, edited by J. G. Webster (Wiley, New York, 1999), p. 64.
- [4] G. Korniss, Z. Toroczkai, M. A. Novotny, and P. A. Rikvold, *Phys. Rev. Lett.* **84**, 1351 (2000).
- [5] A.-L. Barabási and H. E. Stanley, *Fractal Concepts in Surface Growth* (Cambridge Univ. Press, Cambridge, 1995) and references therein.
- [6] D. P. Landau and K. Binder, *Monte Carlo Simulations in Statistical Physics* (Cambridge Univ. Press, Cambridge, 2000).
- [7] W. K. Burton, N. Cabrera, and F. C. Frank, *Phil. Trans. Roy. Soc. (London) Ser. A* **243**, 299 (1951).
- [8] P. A. Rikvold and M. Kolesik, *J. Stat. Phys.* **100**, 377 (2000).
- [9] P. A. Rikvold and M. Kolesik, in preparation.
- [10] J. Marro and R. Dickman, *Nonequilibrium Phase Transitions in Lattice Models* (Cambridge Univ. Press, Cambridge, 1999), Ch. 7.
- [11] H. Guo, B. Grossmann, and M. Grant, *Phys. Rev. Lett.* **64**, 1262 (1990).
- [12] M. Kotrla and A. C. Levi, *J. Stat. Phys.* **64**, 579 (1991).
- [13] A. B. Bortz, M. H. Kalos, and J. L. Lebowitz, *J. Comput. Phys.* **17**, 10 (1975).
- [14] P. Meakin, R. Jullien, and R. Botet, *Europhys. Lett.* **1**, 609 (1986).
- [15] R. Hirsch and D. E. Wolf, *J. Phys. A* **19**, L251 (1986).
- [16] J. Neergaard and M. den Nijs, *J. Phys. A* **30**, 1935 (1997).

TABLE I. The three spin classes that contribute to the interface velocity in the SOS model (column 1), together with the corresponding energy changes resulting from a successful spin flip (column 2, with upper sign corresponding to initial $s = -1$ and lower sign to $s = +1$), the average class populations for general tilt angle ϕ (column 3) and for $\phi = 0$ (column 4), and the contributions to the interface velocity in the y -direction for the hard Glauber dynamic (column 5) and for the soft Glauber dynamic (column 6). In columns 3 and 4, X corresponds to the width parameter $X(T, H)$ for the specific dynamic used, given by Eq. (4) in the general case, Eq. (6) for the hard Glauber dynamic, and $X_0(T) = e^{-2\beta J_x}$ for soft dynamics.

Class	$\Delta E = \Delta E_H + \Delta E_J$	$\langle n(j_s) \rangle$, general ϕ	$\langle n(j_s) \rangle$, $\phi = 0$	$\langle v_y(j_s) \rangle_G$	$\langle v_y(j_s) \rangle_{SG}$
0s	$\mp 2H + 4J_x$	$\frac{1-2X \cosh \gamma(\phi) + X^2}{(1-X^2)^2}$	$\frac{1}{(1+X)^2}$	$\frac{\tanh(\beta H)}{1 + \left[\frac{\sinh(2\beta J_x)}{\cosh(\beta H)} \right]^2}$	$\frac{\tanh(\beta H) X_0^2}{1 + X_0^2}$
1s	$\mp 2H$	$\frac{2X[(1+X^2) \cosh \gamma(\phi) - 2X]}{(1-X^2)^2}$	$\frac{2X}{(1+X)^2}$	$\tanh(\beta H)$	$\frac{1}{2} \tanh(\beta H)$
2s	$\mp 2H - 4J_x$	$\frac{X^2[1-2X \cosh \gamma(\phi) + X^2]}{(1-X^2)^2}$	$\frac{X^2}{(1+X)^2}$	$\frac{\tanh(\beta H)}{1 + \left[\frac{\sinh(2\beta J_x)}{\cosh(\beta H)} \right]^2}$	$\frac{\tanh(\beta H)}{1 + X_0^2}$

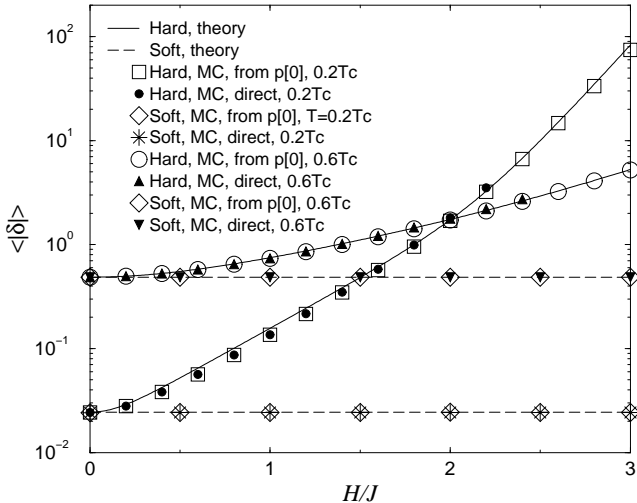


FIG. 1. Average step height $\langle |\delta| \rangle$ vs H for $\phi=0$ at $T=0.2T_c$ and $0.6T_c$, where T_c is the exact Ising critical temperature. Solid curves, obtained as $\langle |\delta| \rangle = 2X/(1-X^2)$ with $X = X_G(T, H)$, are theoretical predictions for the hard dynamic. Dashed lines, similarly obtained with $X = X_0(T)$, are theoretical predictions for the soft dynamic. The MC data are from direct summation over the simulated single-step pdfs (filled symbols) and from $p[0]$ using Eq. (8) (empty symbols). In this and the following figures, the statistical uncertainty is much smaller than the symbol size.

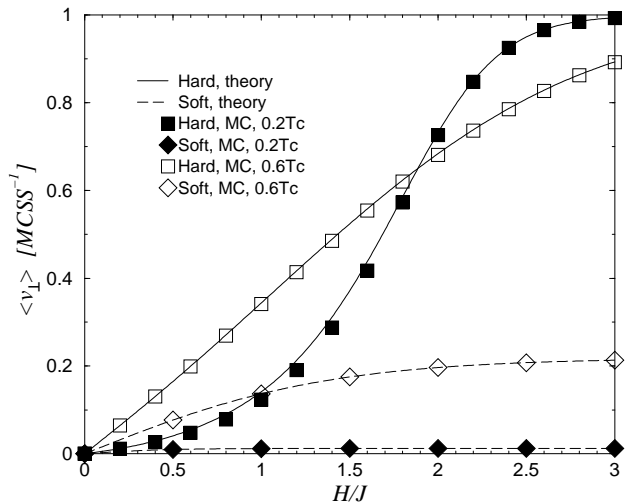


FIG. 2. The perpendicular interface velocity $\langle v_\perp \rangle$ vs H for $\phi = 0$ at $T = 0.2T_c$ and $0.6T_c$. Theoretical results for the hard dynamic are from Eq. (10) (solid curves), with MC data shown as squares. Theoretical results for the soft dynamic are from Eq. (11) (dashed curves), with MC data shown as diamonds.

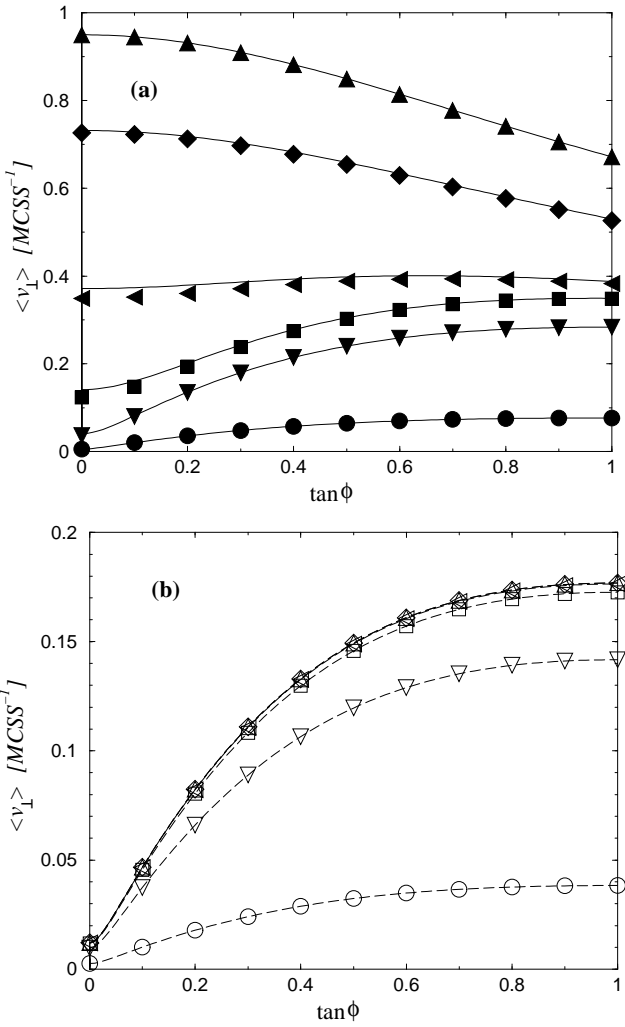


FIG. 3. Angle dependence of the perpendicular interface velocity $\langle v_\perp \rangle$ at $T=0.2T_c$ for (from below to above) $H/J = 0.1, 0.5, 1.0, 1.5, 2.0$, and 2.5 . Curves are theoretical predictions, data points MC results. (a) Hard dynamic. (b) Soft dynamic. On this scale, the soft-dynamic results overlap for $H/J \geq 1.5$.